https://doi.org/10.6113/TKPE.2020.25.2.103

태양광-배터리-수퍼캡을 갖는 직류 홈 그리드의 설계 및 운영

헤리얀토 누르[1], 이동춘†

Design and Operation of DC Home Grid with PV-Battery-Ultracapacitor

Nur A. Heryanto[1] and Dong-Choon Lee†

Abstract

In this study, the design and operating strategy of DC home grid with PV, battery, and ultracapacitor have been discussed, The proposed sizing method can find the optimum size of the battery and PV which can reduce yearly utility energy consumption, whereas the control scheme can maintain the DC-bus voltage level of the DC home grid under different operating conditions, where day or night time operation, load and PV power levels, and the maximum current and state-of-charge of batter are considered. In addition, a supervisory power management strategy has been suggested, and its validity has been verified by HILS (hardware in-the-loop simulation) results.

Key words: Battery, DC home grid, HILS, PV, Ultracapacitor

1. Introduction

The increasing use of solar energy for modern electricity has put DC power at the forefront of systems with integrated grid, energy storage and renewable energy sources. Future homes with rooftop PV and behind-the-meter storage are expected to be DC powered[1]-[3].

A home powered by DC can be regarded as a DC home. In the literature, a DC home with its own renewable energy sources, storage, and load connected to a common DC bus has been oftenly mentioned as a DC nanogrid[4]-[6]. In this regard, a DC home grid can therefore be defined as the DC nanogrid that comprises a DC home.

Meanwhile, hybrid energy storage system has been introduced recently to DC microgrids to improve performances[7]. Combination of battery and ultracap provides an approach to supply pulsating loads effectively. This idea can be brought into application within the DC home grid.

In the literature, the design of the DC home grid can be classified into converter design[4], controller design[5] and sizing of the energy storage[6]. The design approach of the DC home grid is inherently unique to the design targets and problems as different design targets and problems lead to different design approaches and solutions.

In this paper, a design approach for a DC home grid is proposed as in Fig. 1, in which the design output is the optimal battery size to reduce yearly energy consumption from utility. In contrast to the literature[6], the selection of battery chemistry is not discussed in this paper which provides a more general sizing rule of the battery regardless of the chemistry.

Moreover, as load profile and PV generation profile is considered in this paper, the optimal battery size is sensitive to both parameters. This results in different battery size in respect to different load profiles and PV generation profiles.

This paper is the extended version of previous work[8]. For a DC home grid with PV, battery and ultracap, the system profile is described and the sizing of energy storage is elaborated. Basic converter

Paper number: TKPE-2020-25-2-5
Print ISSN: 1229-2214 Online ISSN: 2288-6281
† Corresponding author: dclee@yu.ac.kr, Dept. of Electrical Engineering, Yeungnam University
Tel: +82-53-810-2582 Fax: +82-53-810-4629
[1] Dept. of Electrical Engineering, Yeungnam University
Manuscript received Nov. 11, 2019; revised Dec. 17, 2019; accepted Jan. 4, 2020
— 본 논문은 2019년 전력전자학술대회 태양광논문상 수상논문임

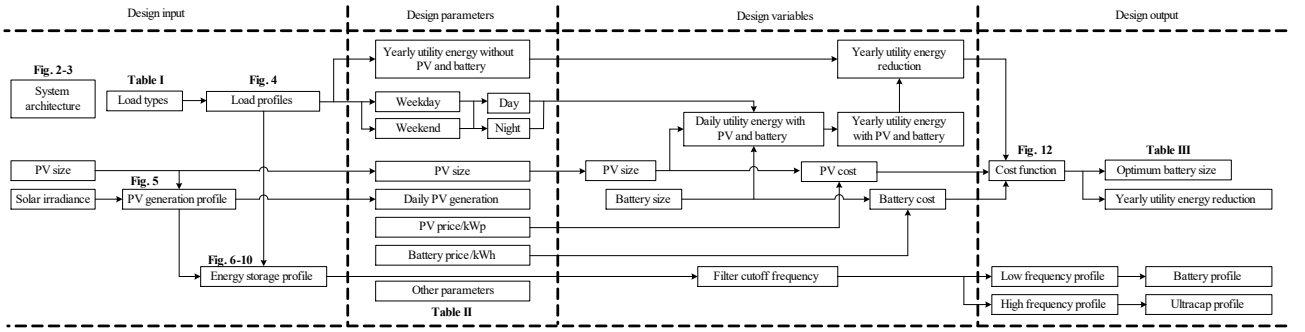

Fig. 1. DC home grid design flowchart.

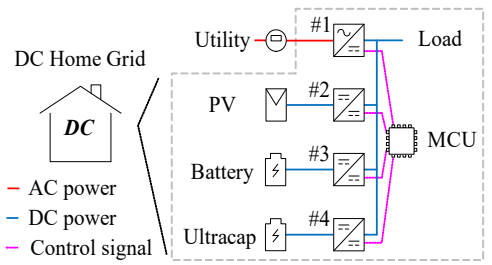

Fig. 2. DC home grid layout.

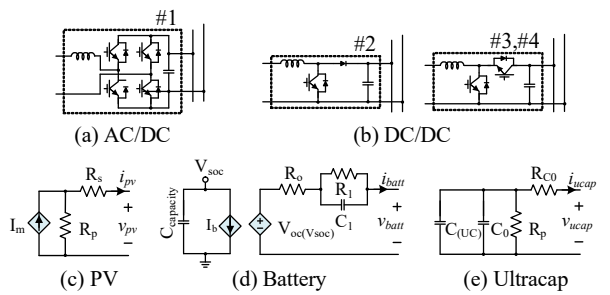

Fig. 3. Circuit models.

circuits are considered as more attention is given to the operating strategy of the whole system. The battery is sized so as to minimize the need of utility power. Finally, by implementing supervisory power management system[7], the operating strategy is verified by HILS.

2. Modeling of DC Home Grid

Fig. 2 shows the layout of the DC home grid, in which an AC/DC converter interfaces with utility and three DC/DC converters interface with PV, battery and ultracap. A single microcontroller unit (MCU) controls all converters entirely.

Fig. 3(a)-(b) show the converter circuits, and Fig. 3(c)-(e) show the equivalent circuits of PV, battery and ultracap[9]-[11]. Advanced converter circuits and controller are available in the literature[4],[5],[12],[13].

TABLE I
LOAD TYPES FOR DC HOME GRID

Power	Description	Power	Description
1x 2000W	Washing machine	1x 100W	Electric rice cooker
1x 2000W	Electric iron	1x 100W	LED TV
1x 1500W	Hair dryer	1x 50W	Electric fan
1x 1000W	Microwave	2x 50W	Smart phone charger
1x 200W	Refrigerator	4x 40W	LED Lighting

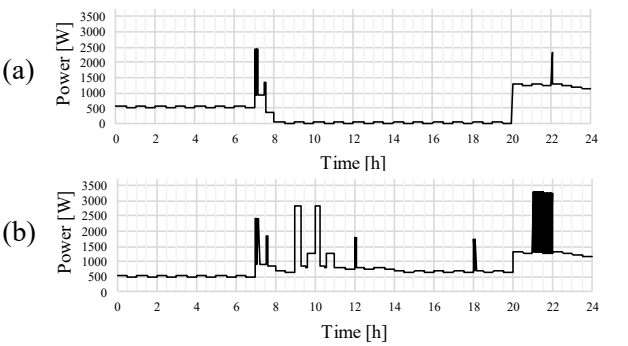

Fig. 4. Load profiles. (a) Weekday, (b) Weekend.

2.1 Load profiles

Load profiles are essential to derive a proper system size, avoiding oversize and undersize cases. Typical loads[14],[15] for a home with electricity consumption below 200 kWh per month are listed in Table I. Fig. 4(a)-(b) show the load profile of typical weekday and weekend, respectively,

2.2 PV generation profile

Solar irradiance (G) is given based on actual measurement[16] and PV output power (P_{PV}) is related by[17]

$$P_{PV}(t) = \eta A G \quad (1)$$

where η is efficiency and A is the area of PV. Fig. 5(a)-(b) shows G and P_{PV} respectively in the case of η=11.25% and A=30m^2.

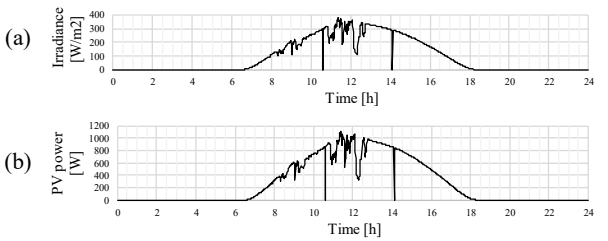

Fig. 5. PV output profile. (a) G, (b) P_{PV}.

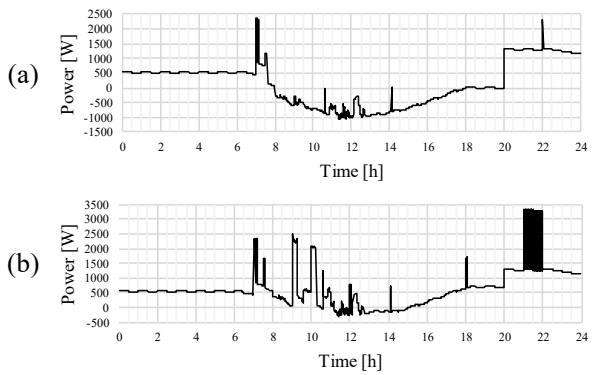

Fig. 6. Profile of P_{ES}. (a) Weekday, (b) Weekend.

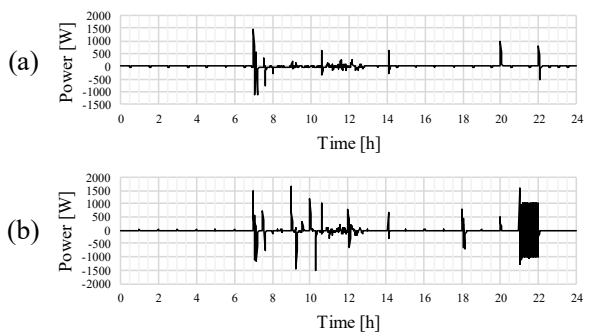

Fig. 7. Profile of $P_{ES,HF}$. (a) Weekday, (b) Weekend.

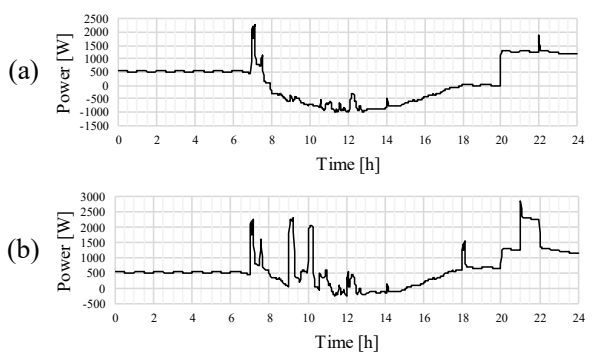

Fig. 8. Profile of $P_{ES,LF}$. (a) Weekday, (b) Weekend.

2.3 Energy storage profile

The energy storage profile is derived from load and PV profiles of which the power, P_{ES}, is expressed as

$$P_{ES} = -\left(P_{PV} - P_{load}\right) \tag{2}$$

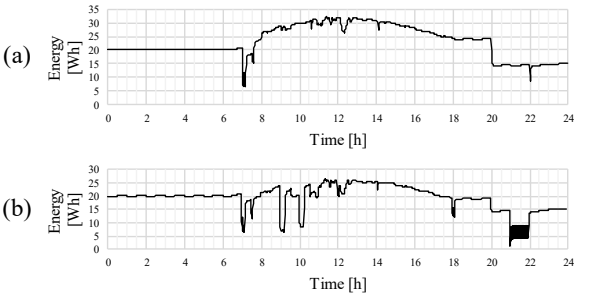

Fig. 9. Profile of $E_{ES,HF}$. (a) Weekday, (b) Weekend.

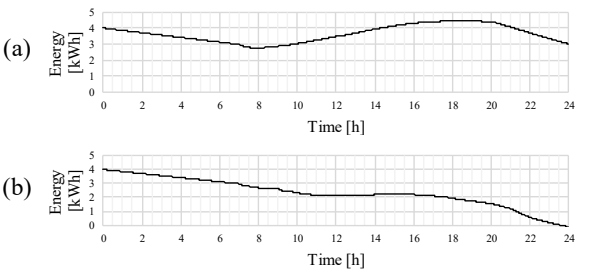

Fig. 10. Profile of $E_{ES,LF}$. (a) Weekday, (b) Weekend.

where the negative sign implies that the excess of PV output power is charged into the energy storage.

Fig. 6 shows the profile of P_{ES} for weekday and weekend, based on (2), P_{load} (Fig. 4) and P_{PV} (Fig. 5).

The profile of P_{ES} in Fig. 6 can be split into two components, the high-frequency ($P_{ES,HF}$) and the low-frequency ($P_{ES,LF}$), related by

$$P_{ES,HF} = \mathrm{HPF}(P_{ES}) \tag{3}$$

$$P_{ES,LF} = P_{ES} - P_{ES,HF} \tag{4}$$

HPF in (3) is a discrete high-pass filter, given as[18]

$$Y_k = \frac{1}{2+\omega_c T}\left(Y_{k-1}\left(2-\omega_c T\right) + 2\left(U_k - U_{k-1}\right)\right) \tag{5}$$

where Y is output, U is input, T is sampling time, ω_c is cutoff frequency and k is number of the sampled data. In theory[7], the battery delivers $P_{ES,LF}$, whereas the ultracap supplies $P_{ES,HF}$.

Fig. 7-8 show $P_{ES,HF}$ and $P_{ES,LF}$ for weekday and weekend, using Eq. (3)-(5), P_{ES} (Fig. 6) and setting T = 60 s, ω_c = 0.01 rad/s.

The stored energy, is described by

$$E_{ES} = E_{ES,0} - \int P_{ES} dt \tag{6}$$

where $E_{ES,0}$ is an initial value. By using Eq. (6), P_{ES} (Fig. 7-8) and setting $E_{ES,HF,0}$ = 20 Wh, $E_{ES,LF,0}$ = 4 kWh, the profiles of E_{ES} are shown in Fig. 9 and 10.

2.4 Utility power profile

When considering power from utility, $P_{utility}$, Eq. (2) is modified into

$$P_{utility} + P_{ES} = -\left(P_{PV} - P_{load}\right) \tag{7}$$

By introducing $P_{utility}$ in Eq. (7), the required power of energy storage can be decreased, which reduces the required capacity, and resultantly, the size of the energy storage. The following section will further develop the sizing of energy storage by considering $P_{utility}$.

3. Sizing of Energy Storage

The energy storage of the DC home grid consists of battery and ultracap. Since the energy capacity of the ultracap is very small compared to that of the battery, energy of the ultracap is negligible in the subsequent sizing equations. However, special consideration will be given to the size of ultracap in the end of this section. A flowchart for sizing the energy storage is shown in Fig. 11.

A cost function is needed to select an optimum size of energy storage in the DC home grid. In this work, the cost function f is defined as

$$f = \min\left(\frac{C_{pv} + C_{batt}}{\Delta E_u}\right) \tag{8}$$

where C_{pv} is the PV costs, C_{batt} is the battery costs, and ΔE_u is the yearly utility energy reduction.

Eq. (8) can be described in more detail as follows:

$$C_{pv} = \lambda_{pv} P_{pv,kWp} \tag{9}$$
$$C_{batt} = \lambda_{batt} E_{batt} \tag{10}$$
$$\Delta E_u = E_{u,0} - E_{u,pv+b} \tag{11}$$
$$E_{u,pv+b} = E_{u,wd} N_{wd} + E_{u,we} N_{we} \tag{12}$$

where λ_{pv} and λ_{batt} are the prices of PV and battery, $P_{pv,kWp}$ is the peak power capacity of PV, E_{batt} is the energy capacity of battery, $E_{u,0}$ and $E_{u,pv+b}$ are the yearly utility energy consumption without and with PV and battery, $E_{u,wd}$ and $E_{u,we}$ are the utility energy consumption with PV and battery for weekday and weekend, N_{wd} and N_{we} are the number of weekdays and weekends in a year, subscripts $_{wd}$ and $_{we}$ relate the variables to weekday and weekend, respectively.

In Eq. (12), $E_{u,wd}$ is calculated from (13)-(18) as

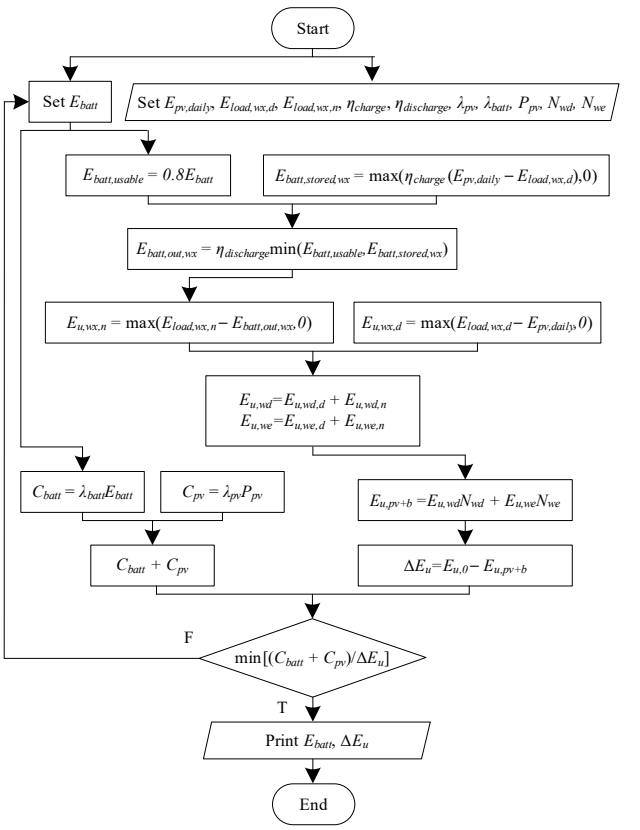

Fig. 11. Flowchart for sizing the energy storage.

$$E_{u,wd} = E_{u,wd,d} + E_{u,wd,n} \tag{13}$$
$$E_{u,wd,d} = \max\left(E_{load,wd,d} - E_{pv,daily}, 0\right) \tag{14}$$
$$E_{u,wd,n} = \max\left(E_{load,wd,n} - E_{batt,out,wd}, 0\right) \tag{15}$$
$$E_{batt,out,wd} = \eta_{discharge} \min\left(E_{batt,usable}, E_{batt,stored,wd}\right) \tag{16}$$
$$E_{batt,usable} = 0.8E_{batt} \tag{17}$$
$$E_{batt,stored,wd} = \max\left(\eta_{charge}\left(E_{pv,daily} - E_{load,wd,d}\right), 0\right) \tag{18}$$

where $E_{u,wd,d}$ and $E_{u,wd,n}$ are $E_{u,wd}$ in respect to day and night, $E_{load,wd,d}$ and $E_{load,wd,n}$ are the energy consumed by load during day and night, respectively, $E_{pv,daily}$ is the daily generated energy from PV, $E_{batt,out,wd}$ is the discharged energy from the battery during the night, $\eta_{discharge}$ and η_{charge} are the discharging and charging efficiency, $E_{batt,usable}$ is the usable capacity of the battery and $E_{batt,stored}$ is the energy stored into the battery. $E_{u,we}$ is then calculated similarly to Eq. (13)-(18).

Table II lists the design parameters used in this work based on load profile[14] in Fig. 4 and PV profile[16] in Fig. 5. Based on Table II, $(C_{pv}+C_{batt})/\Delta E_u$ versus E_{batt} is plotted in Fig. 12. The minimum of the cost function f is found as shown in Fig. 12,

TABLE II
DESIGN PARAMETERS OF DC HOME GRID

Parameter	Unit	Value	Parameter	Unit	Value
$E_{load,wd,d}$	kWh	0.48	$E_{pv,daily}$	kWh	2.3
$E_{load,wd,n}$	kWh	2.3	$E_{u,0}$	kWh	1332
$E_{load,we,d}$	kWh	2.9	η_{charge}		0.9
$E_{load,we,n}$	kWh	2.9	$\eta_{discharge}$		0.9
$P_{pv,kWp}$	kWp	3/5	λ_{pv}	\$/kWp	770
N_{wd} /N_{we}	260 /105		λ_{batt}	\$/kWh	513

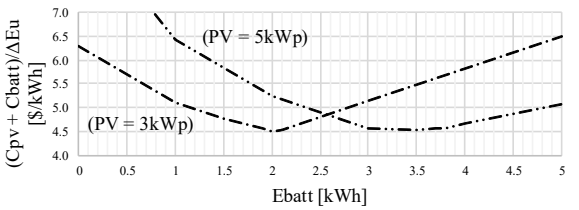

Fig. 12. Plot of $(C_{pv}+C_{batt})/\Delta E_u$ versus E_{batt}.

TABLE III
SUMMARY OF SIZING RESULTS

	Parameters	Size	Cost
Case I	PV	3 kWp	\$2,310
	Battery	2 kWh	\$1,026
	Ultracap	160V/21Wh	\$1,026
	Total cost		\$4,362
	ΔE_u		741kWh
Case II	PV	5 kWp	\$3,850
	Battery	3.5 kWh	\$1,795
	Ultracap	160V/21Wh	\$1,026
	Total cost		\$6,671
	ΔE_u		1250kWh

which its minimum point is the optimal size of the battery capacity.

Table III lists a summary of the sizing which stems from Fig. 12. The energy capacity of the ultracap is selected from the profiles of $P_{ES,HF}$ described in section 2.3. The nominal voltage of ultracap is selected considering a 300-350 V_{DC} bus voltage level.

4. Control of DC Home Grid

In this section, the control strategy of the DC home grid is discussed. There exist abundant control methods of DC microgrid which can be applied to the

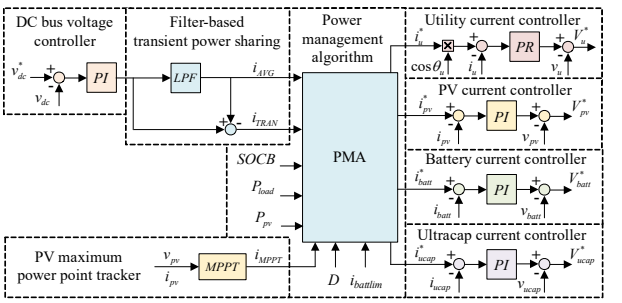

Fig. 13. Control structure.

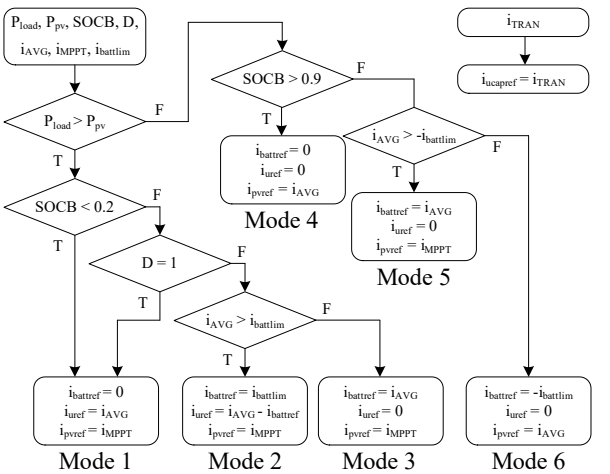

Fig. 14. Flowchart of PMA.

DC home grid. Among them, the newly introduced supervisory power management system[7] is adopted.

Fig. 13 shows the control structure for DC home grid with PV-battery-ultracap derived from the supervisory power management system. The DC-bus voltage controller is a PI controller, of which output is a reference current that is shared among utility, PV, battery and ultracap current controller through a power management algorithm (PMA).

Following the output of the DC-bus voltage controller, there is a filter-based transient power sharing that produces i_{AVG} and i_{TRAN}. The value of i_{AVG} is set as utility, PV or battery reference current according to the PMA, while the value of i_{TRAN} is considered as the ultracap reference current so that the ultracap provides or absorbs power during transient state of DC-bus voltage. Each current controller is a PI type, except the utility current controller which is a PR type.

With electricity price and energy arbitrage excluded, the operating scheme of DC home grid can be simpler. Fig. 14 shows the flowchart of the PMA which can be used to operate the DC home grid. By default, the PMA assigns i_{TRAN} to the ultracap

reference current. Then, by considering PV power (P_{pv}), load power (P_{load}), battery state-of-charge (SOCB), battery current limit ($i_{battlim}$) and time of operation (D = 0 for night and D = 1 for day), i_{AVG} is assigned to PV, utility, or battery reference current according to the flowchart. The PV reference current is normally set as the output of the PV MPPT controller, except when the battery is fully charged (Mode 4) or the battery charges at its current limit (Mode 6). The battery is charged under Mode 5 and 6 and discharged under Mode 2 and 3. The battery is idle under Mode 1 as the load is mainly supplied by utility; it happens either when battery SOC is depleted during the night or when P_{load} is higher than P_{pv} during the day (D = 1).

5. HILS Results

The DC home grid is modeled in NI PXI platform and simulated in a real time. The simulation setup in this work is considered using Controller-HIL configuration[19]. The circuit model in Fig. 3 is built in LabView and compiled into NI PXI hardware. Loads are lumped into an equivalent constant power load (CPL), where a dependent current source (i.e., $i_{load} = P_{load}/V_{dc}$) emulates the load profile. The control scheme and PMA described in section 4 are implemented by DSP TMS320F28335. The cutoff frequency of the LPF in the control structure in Fig. 13 is selected as 0.04775 Hz.

Table IV shows the HILS parameters and scenario to test the control scheme of the DC home grid with PV-battery-ultracap. Utility is considered having a single-phase AC voltage of 220 V_{rms} with frequency 60 Hz. The DC bus rated voltage, V_{dc}, is considered as 350 V, which fulfills $V_{dc} \geq (\sqrt{2})V_{rms}$. The rated voltage of the DC-DC converter input interfacing with PV, V_{pv}, is selected as 150 V, which considers five PV panels in series, each voltage is 30 V at maximum power point. The rated voltage of the battery storage, V_{batt}, is 120 V considering five 24 V battery packs in series. Ultracap voltage, V_{ucap}, is selected as 160 V based on 160V/6F ultracap module.

The scenario consists of ten cases; cases I-V represents the night scenario (D = 0) and cases VI-X represents the day scenario (D = 1). The value of SOCB, P_{load}, and i_{MPPT} are varied to test the operating scheme of the DC home grid as previously described in section 4.

TABLE IV
HILS SCENARIO

Parameters			$V_{utility}$	$f_{utility}$	V_{dc}	V_{pv}	V_{batt}	V_{ucap}
			220V_{rms}	60Hz	350V	150V	120V	160V
Case	D	Mode	P_{load} [W]	SOCB	i_{MPPT} [A]	P_{pv} [W]	P_{batt} [W]	$P_{utility}$ [W]
I	0	1	0	0.5	0	0	0	0
II	0	3	600	0.5	0	0	600	0
III	0	2	2400	0.5	0	0	1150	1250
IV	0	3	600	0.5	0	0	600	0
V	0	1	600	0.1	0	0	0	600
VI	1	1	600	0.1	0	0	0	600
VII	1	1	600	0.1	4	600	0	0
VIII	1	5	600	0.1	8	1200	-600	0
IX	1	1	2400	0.1	8	1200	0	1200
X	1	5	600	0.1	8	1200	-600	0

First, the system is tested under night scenario as in cases I-V. In these cases, P_{PV} is not available. Initially, there is no load as in case I. Then, a 600 W CPL is switched on which is supplied by the battery as in case II. When P_{load} increases to 2400 W as in case III, the battery discharges at its limit value and the utility supplies power to maintain the DC bus voltage at its reference value. When battery SOC is depleted as in case V, the load is fully supplied by utility.

Next, day scenario is considered as shown in cases VI-X. During the day, when P_{pv} is not available, the load is supplied by utility as in case VI. When P_{pv} equals to P_{load}, utility power is no longer needed as in case VII. When P_{pv} is higher than $P_{load,}$ the excess of PV power is charged into battery as in case VIII. The battery stops charging when P_{load} is higher than P_{pv} as in case IX.

Fig. 15 shows the power responses and DC bus voltage of the DC home grid from real-time simulation for the scenario as listed in Table IV.

The difference of the power management in this paper from the conventional supervisory power management system[7] is that time-of-use (ToU) tariffs of electricity pricing scheme is not considered in this paper, which simplifies the implemented PMA in Fig. 15. Furthermore, the controller type of converter interfacing with utility in this paper is a PR type whereas the conventional scheme uses hysteresis controller.

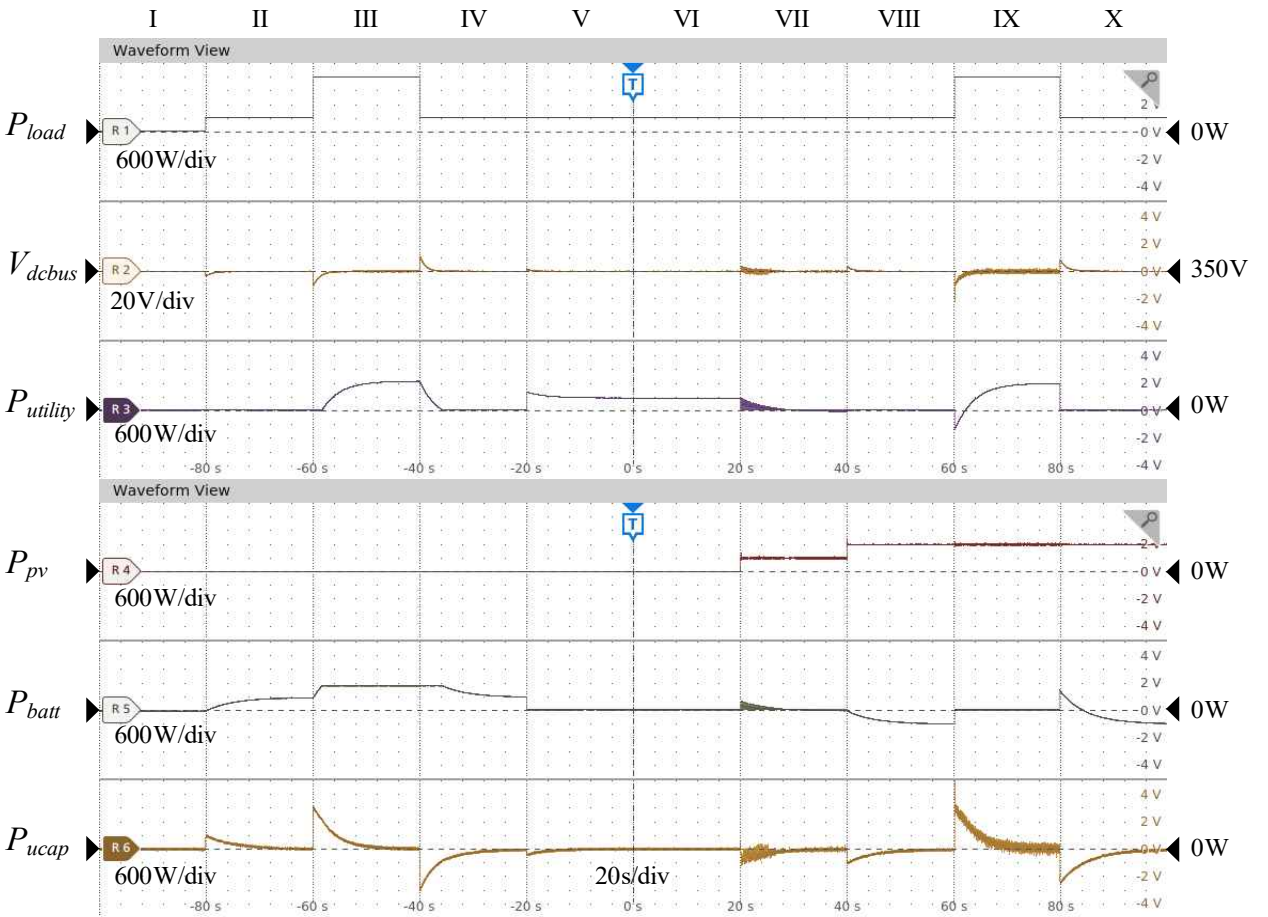

Fig. 15. Responses of power in HILS scenario.

From the HILS result in Fig. 15, it is shown that the power management algorithm has worked under the scenario of Table IV, despite oscillations appear in case VII and IX, which needs further investigations.

6. Conclusion

In this paper, the design and operating strategy of a DC home grid with PV-battery-ultracap have been discussed. The circuit equivalent model, load profile, PV power, energy storage profile and sizing scheme have been developed. The control structure based on supervisory power management scheme has been applied to the HIL system, where in this paper ToU pricing is not considered and only essential power management algorithm is considered. From the HILS results, the validity of the control scheme has been verified.

This research was supported by Korea Electric Power Corporation.(Grant number : R18XA06-35).

References

[1] D. Boroyevich, I. Cvetkovic, D. Dong, R. Burgos, F. Wang, and F. Lee, "Future electronic power distribution systems a contemplative view," in *Proc. 2010 12th Int Conference on Optimization of Electrical and Electronic Equipment, Basov*, pp. 1369-1380, 2010.

[2] A. Riccobono, M. Ferdowsi, J. Hu, H. Wolisz, P. Jahangiri, D. Muller, R. W. D. Doncker, and A. Monti, "Next generation automation architecture for DC smart homes," in *Proc. 2016 IEEE Int. Energy Conference (ENERGYCON), Leuven*, pp. 1-6, 2016.

[3] L. Mackay, N. H. van der Blij, L. R. Elizondo, and P. Bauer, "Toward the universal DC distribution system," *Electric Power Components and Systems*, 45:10, pp. 1032-1042, 2017.

[4] W. Hassan, S. Gautam, D. D. Lu, and W. Xiao, "Analysis, design, and experimental verification of high step-up DC-DC converter to interface renewable energy sources into DC nanogrid," in *Proc. 2019 IEEE Int. Conference on Industrial Technology (ICIT), Melbourne*, pp. 1649-1654, 2019.

[5] T. L. Nguyen and G. Griepentrog, "Modeling, control and stability analysis for a DC nanogrid system," in

Proc. 2018 19th IEEE Workshop on Control and Modeling for Power Electronics (COMPEL), Padua, pp. 1-8, 2018.

[6] M. C. di Piazza, M. Luna, M. Pucci, G. L. Tona, and A. Accetta, "Electrical storage integration into a DC nanogrid testbed for smart home applications," in *Proc. 2018 IEEE Int. Conference on Environment and Electrical Engineering and 2018 IEEE Industrial and Commercial Power Systems Europe (EEEIC / I&CPS Europe), Palermo*, pp. 1-5, 2018.

[7] S. Kotra and M. K. Mishra, "A supervisory power management system for a hybrid microgrid with HESS," *IEEE Trans. on Industrial Electronics*, Vol. 64, No. 5, pp. 3640-3649, May 2017.

[8] N. A. Heryanto and D. C. Lee, "Bus voltage regulation of DC home grid with PV-battery-ultracap," in *Proc. 2019 Power Electronics Annual Conference*, pp. 467-468, Jul. 2019.

[9] M. G. Villalva, J. R. Gazoli, and E. R. Filho, "Comprehensive approach to modeling and simulation of photovoltaic arrays," *IEEE Trans. on Power Electronics*, Vol. 24, No. 5, pp. 1198-1208, May 2009.

[10] M. Chen and G. A. Rincon-Mora, "Accurate electrical battery model capable of predicting runtime and I-V performance," *IEEE Trans. on Energy Conversion*, Vol. 21, No. 2, pp. 504-511, Jun. 2006.

[11] P. J. Grbovic, P. Delarue, P. Le Moigne, and P. Bartholomeus, "Modeling and control of the ultracapacitor -based regenerative controlled electric drives," *IEEE Trans. on Industrial Electronics*, Vol. 58, No. 8, pp. 3471-3484, Aug. 2011.

[12] Y. C. Jeung, D. D. Le, and D. C. Lee, "Analysis and design of DC-bus voltage controller of energy storage systems in DC microgrids," *IEEE Access*, Vol. 7, pp. 126696-126708, 2019.

[13] Y. C. Jeung and D. C. Lee, "Voltage and current regulations of bidirectional isolated dual-active-bridge DC/DC converters based on a double-integral sliding mode control," *IEEE Trans. on Power Electronics*, Vol. 34, No. 7, pp. 6937-6946, Jul. 2019.

[14] S. B. Lee, W. J. Cho, and K. S. Lee, "Prediction of electrical load profile for use in simulating the performance of residential distributed generation systems," *Korean Journal of Air-Conditioning and Refrigeration Engineering*, Vol. 23, No. 4, pp. 265-272, Apr. 2011.

[15] S. J. Noh, S. J. Lee, S. W. Lee, and K. H. Kim, "Power demand pattern analysis for electric appliances in residential and commercial building," *Journal of Industrial Technology*, Vol. 30A, pp. 9-15, 2010.

[16] Bureau of Meteorology, *One minute dolar data*, Australian Government. [Online]. Available: http://www.bom.gov.au /climate/data/oneminsolar/about-IDCJAC0022.shtml. [Acce ssed Dec. 19, 2019].

[17] R. Ehrlich and H. A. Geller, *Renewable Energy : A First Course*, CRC Press, pp. 260, 2017.

[18] H. P. Hsu, *Schaum's Outline Series : Signals and Systems*, McGraw-Hill, 2011.

[19] D. D. To, D. D. Le, and D. C. Lee, "Development of hardware in-the-loop simulation system for testing power management of DC microgrids based on decentralized control," *The Transactions of the Korea Institute of Power Electronics*, Vol. 24, No. 3, pp. 191-200, Jun. 2019.

Nur A. Heryanto

He received B.S. degree in electrical power engineering from Institut Teknologi Bandung, Bandung, Indonesia in 2016. He worked as a Power Engineer at PT Len Industri (Persero), Indonesia, from 2016 to 2017. He is currently working towards the M.S./Ph.D. degree with the Department of Electrical Engineering, Yeungnam University, Gyeongsan, South Korea.

Dong-Choon Lee

He received his B.S., M.S., and Ph.D. degrees in Electrical Engineering from Seoul National University, Seoul, Korea, in 1985, 1987, and 1993, respectively. He was a Research Engineer with Daewoo Heavy Industry, Korea, from 1987 to 1988. Since 1994, he has been a faculty member in the Department of Electrical Engineering, Yeungnam University, Gyeongsan, Korea. As a Visiting Scholar, he joined the Power Quality Laboratory, Texas A&M University, College Station, TX, USA, in 1998; the Electrical Drive Center, University of Nottingham, Nottingham, UK, in 2001; the Wisconsin Electric Machines and Power Electronic Consortium, University of Wisconsin, Madison, WI, USA, in 2004; and the FREEDM Systems Center, North Carolina State University, Raleigh, NC, USA, from September 2011 to August 2012. He served as the President of the Korean Institute of Power Electronics in 2019.